

The Eurasia Proceedings of Science, Technology, Engineering & Mathematics (EPSTEM), 2023

Volume 22, Pages 1-14

ICBASSET 2023: International Conference on Basic Sciences, Engineering and Technology

Mathematical Analyzing of Laser Triangulation System without Scheimpflug Condition via C++ and Qt Framework

Orkun KASAPOGLU

Baykal Machinery

Tugba BILGIN

Baykal Machinery

Abstract: In this paper, the mathematical characteristics of a laser triangulation system have been analyzed without considering Scheimpflug condition. The system parameters have been investigated and detailed information about the behavior of the system due to the changing some initial parameters just before designing the profile measurement system have been obtained. To be able to evaluate the system, C++ and Qt framework have been used for calculation of multi-dimensional arrays and visualization of the results to investigate the system parameters. The characteristics of the triangulation systems (both for our model and the model that proposed by Lamott and Noll, 2011) and characteristics of laser beam (laser beam thickness change for given measurement field range) for different laser sources with different wavelengths have been investigated. After analyzing the parameters of the triangulation system successfully, an adjustable system will be built in the laboratory to be able to get a better understanding the usage of this system in both 2D and 3D laser cutting systems.

Keywords: Laser Triangulation, Image Processing, C++, Qt

Introduction

Laser triangulation is a widely used measurement technique that involves projecting a laser beam onto a surface and measuring the distance to the surface based on the reflected light. This technique is commonly used in various applications such as 2D/3D scanning, robotics, quality control, and machine vision. The basic principle of laser triangulation is use the position of the reflected light spot to calculate the distance to the surface, based on the angle between the laser beam and the sensor or camera.

Traditionally, laser triangulation systems are designed on the Scheimpflug condition, which is a geometric principle (Fig. 1) that ensures that the image plane, lens plane, and the object plane are intersecting in one line. This condition is necessary to achieve sharp focus and accurate measurements, especially over long distances and at steep angles. However, strictly adhering to the Scheimpflug condition can be challenging, especially in complex or non-standard measurement scenarios.

In recent years, there has been growing interest in the alternative approaches to laser triangulation that do not strictly rely on the Scheimpflug condition. These approaches aim to improve the flexibility, simplicity, and robustness of laser triangulation systems, while still maintaining acceptable levels of accuracy and precision. This article is related with the exploration of the principles and practical considerations of laser triangulation without Scheimpflug condition, and highlights some of the advantages and limitations of this approach.

The characteristic curve of laser triangulation has been discussed for both Lamott and Noll's and our system. Related systems have plenty of application are from thickness measurements of rolled sheets to flatness

- This is an Open Access article distributed under the terms of the Creative Commons Attribution-Noncommercial 4.0 Unported License, permitting all non-commercial use, distribution, and reproduction in any medium, provided the original work is properly cited.

- Selection and peer-review under responsibility of the Organizing Committee of the Conference

measurements of heavy plates or coordinate-measuring machines to the straightness and profile measurements of rails (Donges & Noll, 2015).

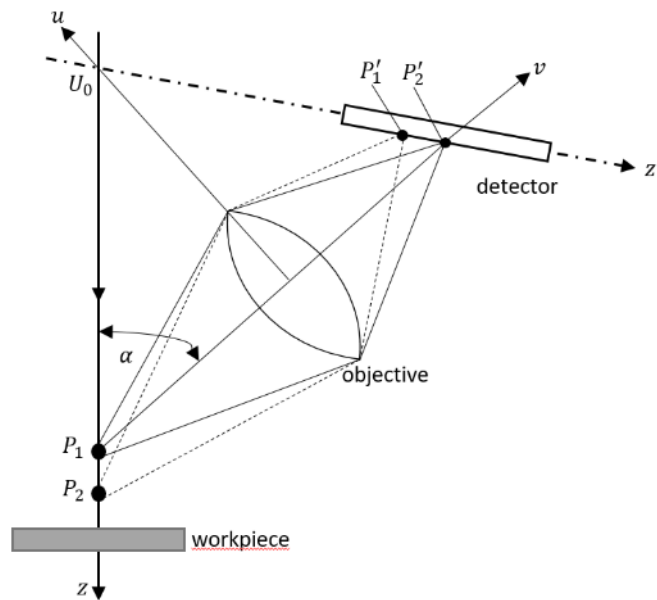


Figure 1. Imaging geometry for laser triangulation including Scheimpflug condition (Lamott & Noll, 2011).

Laser Triangulation without Scheimpflug Condition

Basic Principles

Laser triangulation without Scheimpflug condition is based on the same fundamental principle as traditional laser triangulation (see Fig. 2): the distance to a surface can be determined by measuring the angle in between projected laser beam and the reflected light or calculating the intersection point components for the imaging axis between projected light. However, in this case, the position of the sensor or camera is not necessarily aligned with the image plane and the lens plane. Instead, the sensor or camera is positioned at an angle to the image plane, which allows for more flexible positioning and easier alignment.

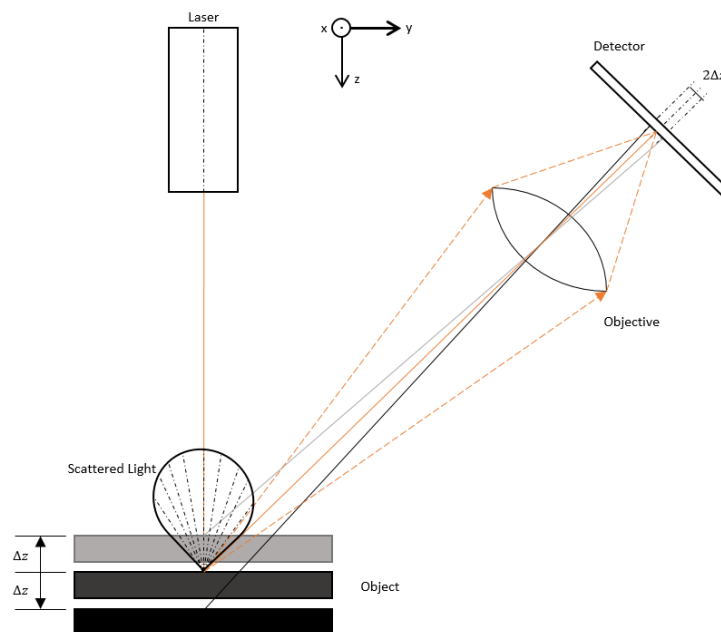


Figure 2. Our laser triangulation system without Scheimpflug condition.

To achieve accurate and precise measurements without the Scheimpflug condition, several factors need to be considered. Firstly, the position and orientation of the sensor or camera relative to the laser beam and the surface need to be carefully controlled and calibrated. This can be achieved using specialized mounting hardware, calibration targets, and software algorithms that compensate for any misalignments or distortions. Secondly, the characteristics of the laser beam and CCD or CMOS sensor need to be optimized according to the requirements for each specific applications. This characteristic includes laser wavelength, laser power, the resolution and sensitivity of the sensor or camera, the spot size and spot shape of the laser, the distance in between whole components to each other relatively and the angle of the measurement.

Advantages and Limitations

Laser triangulation without Scheimpflug condition offers several advantages over traditional laser triangulation. It allows for more flexible and adaptable measurement systems that can be tailored to specific applications and requirements. This can be particularly useful in scenarios where the object being measured is not flat or is difficult to access, or when the measurement system needs to be integrated into a larger system or process.

Laser triangulation without Scheimpflug condition can be easier to set up and use compared to traditional systems. There is no need to precisely align the sensor or camera with the image and lens planes, which can be time-consuming and difficult. Additionally, the reduced complexity of the measurement system makes it more robust and less prone to errors or failures. However, this method is a promising and emerging approach that offers new possibilities and opportunities for laser-based measurement systems. With careful consideration of the basic principles, advantages, and limitations, it can be a valuable tool for a wide range of applications in industry, research, and beyond.

Methods

Programming and Visualization

A desktop application has been developed during this study to be able to analyze the system models with the variation of the some critical parameters. Application contains two different user interfaces. First one is for the visualization of the system characteristics according to system parameters supplied by user. Second one is dedicated for 3D investigations and it is derived from an example from Qt Framework. The screenshots of the application user interfaces are given in below (Fig. 3 and Fig. 4 for 2D and 3D outputs respectively).

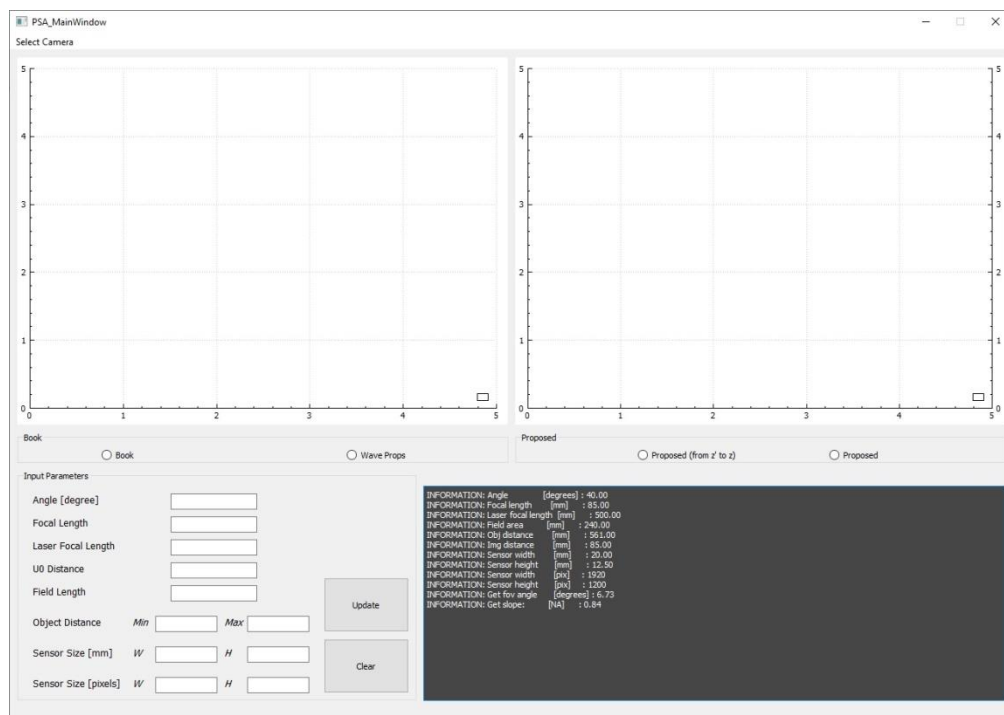


Figure 3. User interface for 2D and system parameters of the developed application.

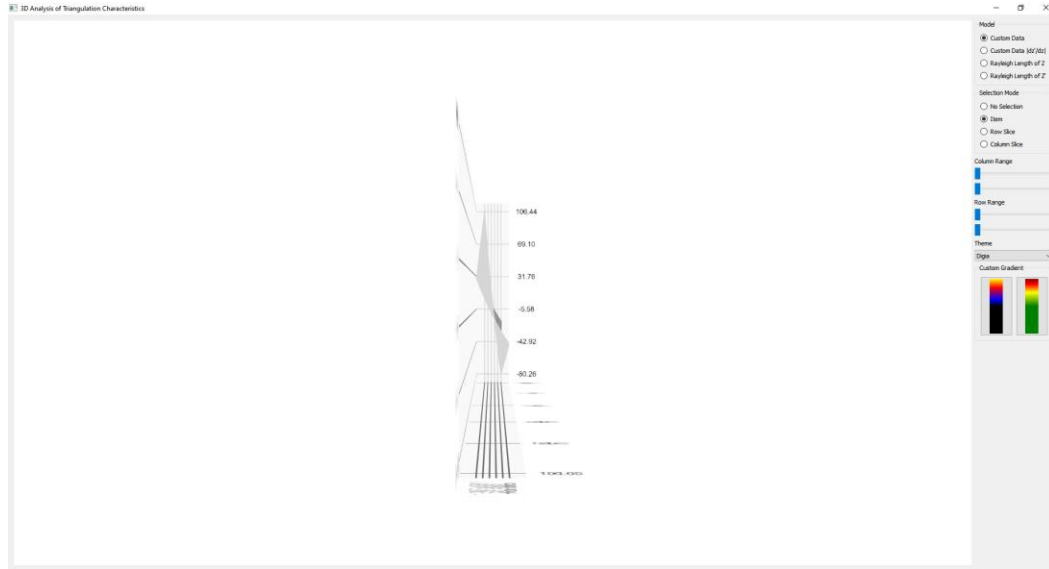


Figure 4. User interface for 3D of the system parameters.

The application has a default parameter list, which is given Figure 3, but it is of course allows to change parameters and all changings affects the behavior of the system.

Mathematical Equation

In this paper, the mathematical model of the laser triangulation without Scheimpflug condition is extracted from the simple hypotenuse representation of the z -coordinates from the imaging geometry of the lens and the camera. Here is the characteristic equation of our system (derivation of this equation is not given):

$$z'(z) = zm_L f \frac{\frac{-1}{d\sqrt{1+m_L^2}}}{1+z\left(\frac{1}{d\sqrt{1+m_L^2}}\right)} \quad (1)$$

Here we can see, $z = 0$ when $z' = 0$ and $z < 0$ when $z' > 0$ (and vice versa). d is the distance from the lens to the $z = 0$ point, f is the focal length of the imaging lens, and m_L is the slope of the laser beam relative to the imaging axis. This equation has extracted from intersection points of the lines those are representing the projected and the reflected light.

Without Scheimpflug condition, the system becoming simple imaging system tilted with a triangulation angle. It is still non-linear for some angles. Linearity of the system directly related with the triangulation angle and increasing of the angle makes system more linear. Optimum triangulation angle needs to be defined according to the equipment via test and/or simulation.

Characteristic Curve of Triangulation Sensors

There is an equation related with the relationship in between the position of the light spot on the test object and the location of the imaged light spot at the detector. The location of the light spot on the straight line described by via this equation and determines unequivocally the position of the imaged light spot. Following equation represents a light spot at the position z would be projected onto the detector plane at the corresponding point z' (Donges and Noll, 2015):

The method that has been given in the Eq. (2) is finding the sensor points from given z -distances while the method has been given in this paper is finding the z -distances from the given z' sensor points.

$$z'(z) = m_L f \sqrt{1 + \left(m_L - \frac{u_0}{f}\right)^2} \cdot \frac{\left(\frac{z}{\sqrt{1 + m_L^2}}\right)}{\left(\frac{z}{\sqrt{1 + m_L^2}} + \frac{u_0}{m_L} - f\right) \left(m_L - \frac{u_0}{f}\right)} \quad (2)$$

The characteristic curves of the both equations and the $|dz'/dz|$ sensitivity changes are shown in Fig. 3 and Fig. 4.

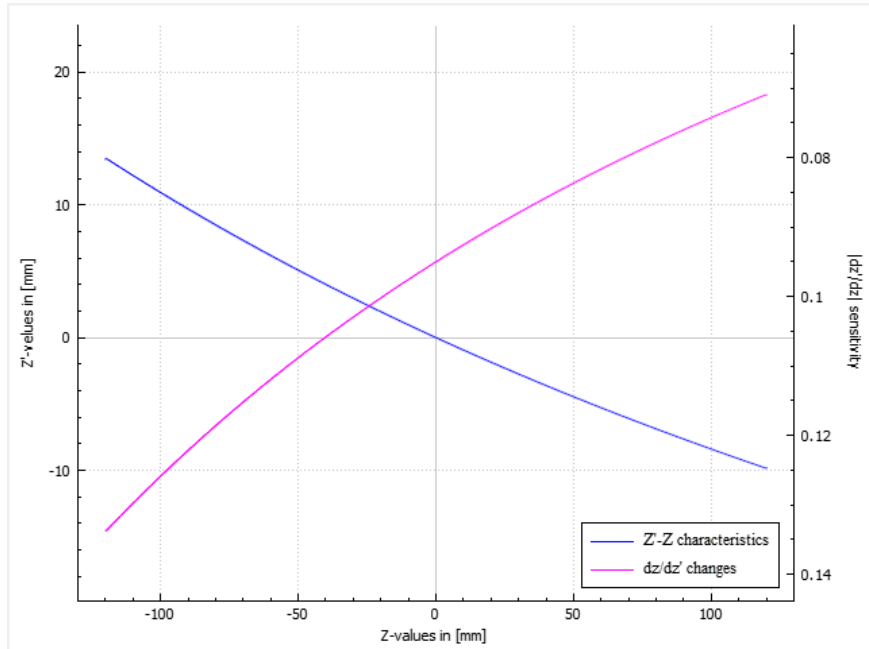


Figure 5. Coordinate of the image spot z' and the sensitivity (dz'/dz) as a function of the illuminated spot position z (Lamott and Noll, 2011).

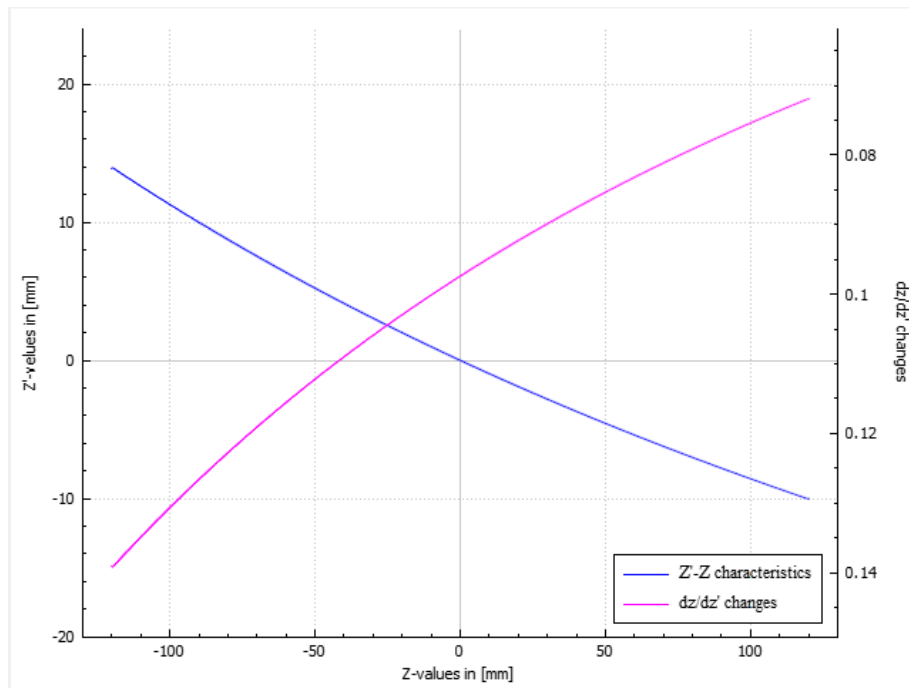


Figure 6. Same plotting for method which has been given in this paper.

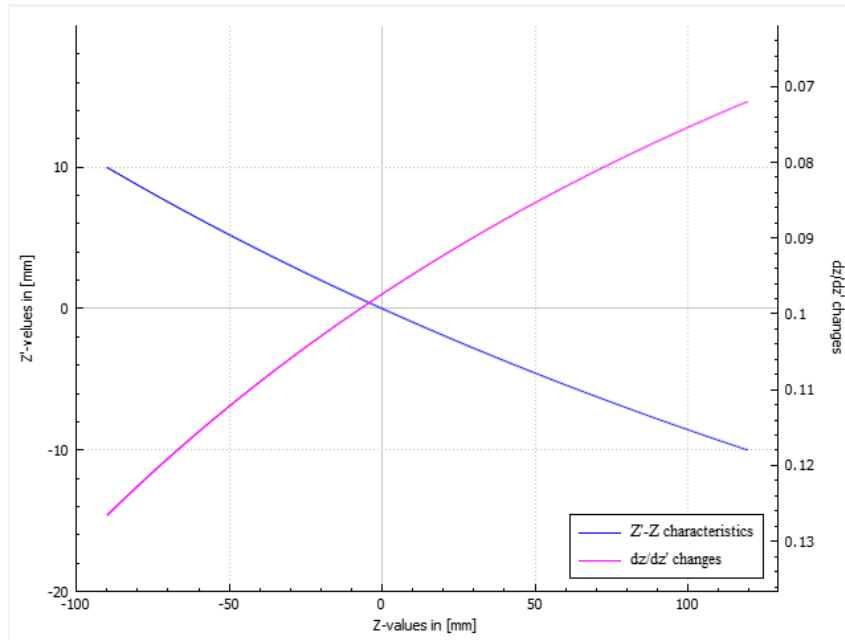


Figure 7. Same plotting for $z(z')$ in our model. It can be seen that the range is limited with the sensor size.

Table 1. Values used in the equations (from Donges & Noll, 2015).

Name	Unit	Value
Angle	Degrees	40
Focal Length	mm	85.00
Field Area	mm	240
U0	mm	561

According to the graphs, which are given in above, it is obviously clear that the results are nearly same for both Lamott and Noll's and our approaches.

Measuring Fields of Triangulation Sensor

Measuring field of a triangulation sensor gives the measurable x-ranges and the z-depth ranges for measurement distances. For example, measuring field for the Wenglor MSL124 2D/3D Profile Sensor which is used in the industrial applications can be seen from Fig. 6.

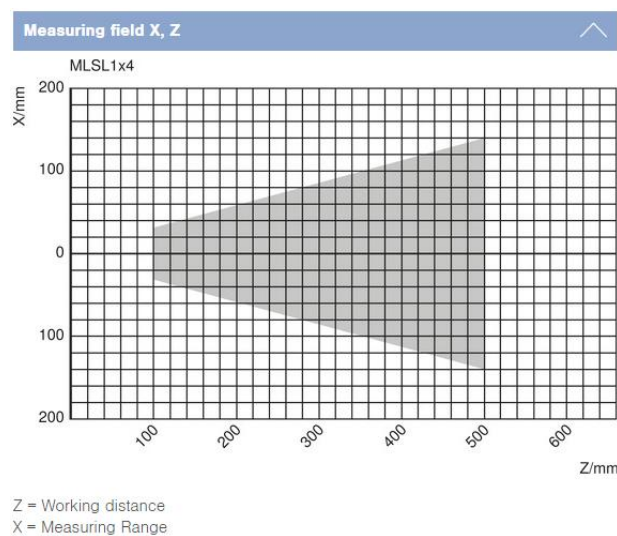


Figure 8. Measuring field for the Wenglor MSL124 2D/3D profile sensor (Wenglor MSL124).

Fig. 8 telling us, measurable x-length is depends on the distance in between the measurement plane and sensor. For example, the sensor can measure 60mm length when the sensor placed at from 100mm away from the measurement plane and 280mm length when it placed 500mm away from the measurement plane.

The measuring field of our method based on the Donges and Noll's parameters (Table 1) is given in Figure 9. It can be seen that our system can measure 14mm length when the sensor placed at from 100mm away from the measurement plane and 74mm length when it placed 500mm away from the measurement plane (Fig. 9). And Fig. 10 is showing that the measurable depth distance of the system when the camera has a distance from 100mm to 500mm to the surface being measured.

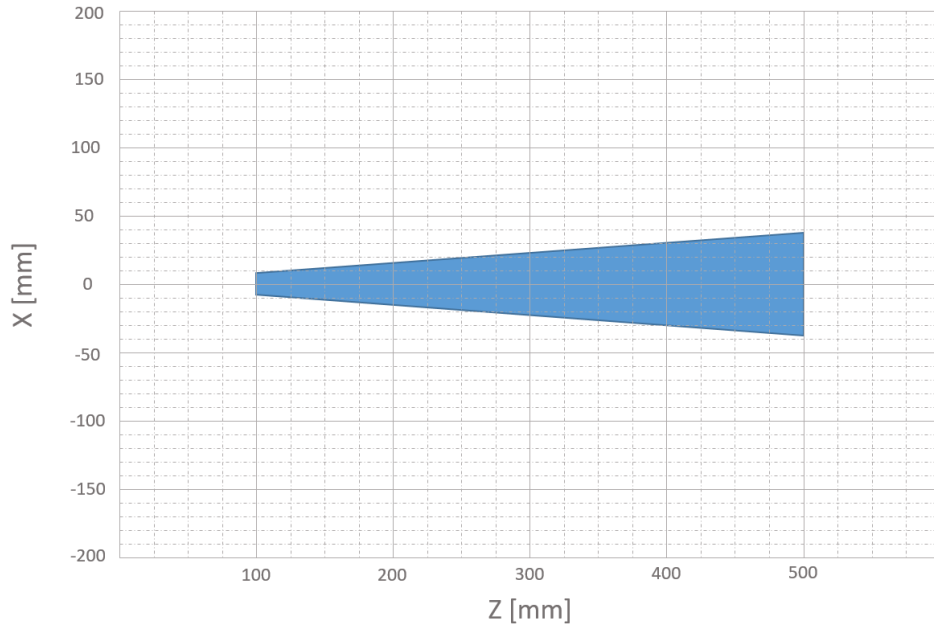


Figure 9. Measuring field for the method that has been given in this paper using with parameters from Donges and Noll ($U_0 = 561\text{mm}$, focal length = 85mm , sensor size $h = 10.25\text{mm}$).

The measuring field for z-depth values mean that the measurable range from the specific measurement distance d related to the sensor size and imaging parameters and can be seen in Fig. 10.

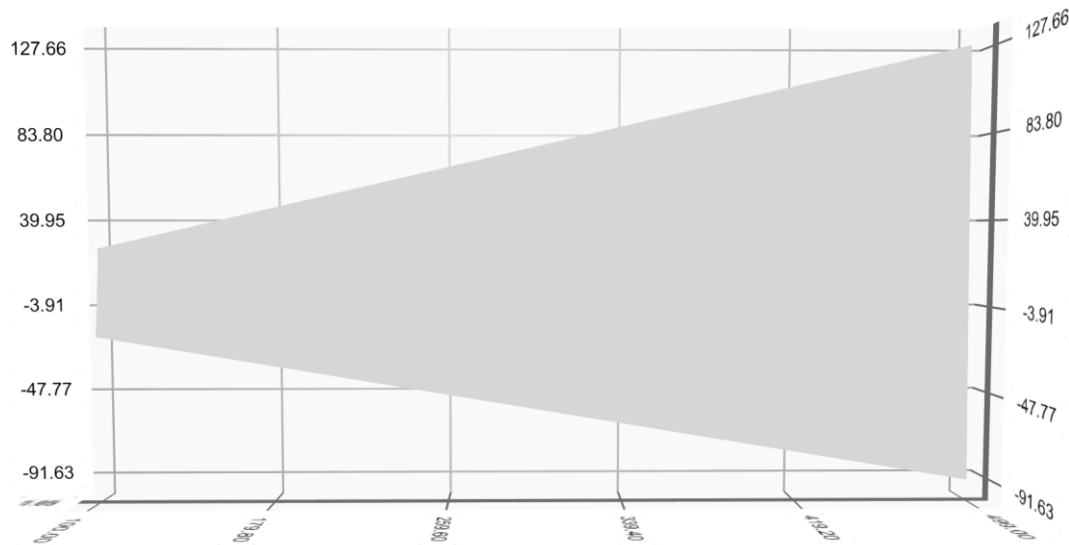


Figure 10. Measuring depth field related to measurable z-depth from the measuring distances of the model.

The current values that is used in these equations are taken from (Donges & Noll, 2015). However, in the implementation of the laser triangulation without Scheimpflug condition is limited due to the imaging components in the market such as industrial cameras and objective lenses.

Laser Beam Characteristics

Laser beam characteristics are determined generally by the type of the laser source and the shaping optics. To achieve high resolving power in triangulation, the diameter of the laser beam should be kept as small as possible at the surface being measured (Donges and Noll, 2015).

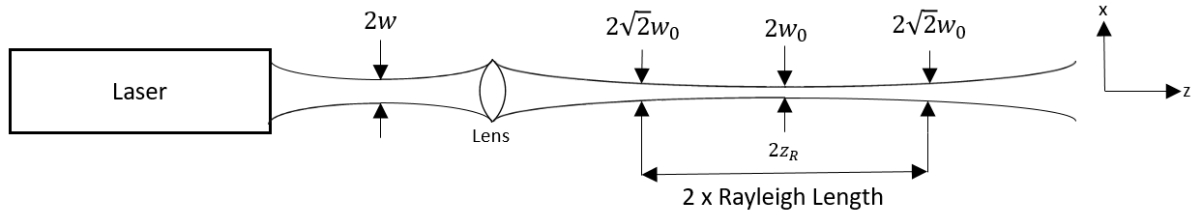


Figure 11. Propagation of a Gaussian laser beam (diagram is not to scale) (Donges & Noll, 2015).

The laser beam is focused with a lens. The beam waist diameter at the surface being measured amounts $2w$. For the calculation of laser beam diameter at the focus of the laser source (Donges and Noll, 2015):

$$2w_0 = \frac{2\lambda}{\pi w} f_F \quad (3)$$

where λ is the wavelength of the laser source, $2w$ is beam waist diameter of the laser beam in front of the focusing lens, $2w_0$ is diameter of the laser beam at the focus and f_F is focal length of the focusing lens. The Rayleigh length of a Gaussian laser beam indicates the distance along the beam, from the focusing position, at which the diameter is larger than the focus diameter by a value $\sqrt{2}$, see Fig. 11. For the Rayleigh length z_R (Donges & Noll, 2015):

$$z_R = \frac{\pi}{\lambda} w_0^2 \quad (4)$$

The Gaussian beam diameter $2w_0$ is plotted as a function of $2z_R$ for 660nm and 520nm, according to Eq. (4), can be seen in Fig. 12 (Donges & Noll, 2015).

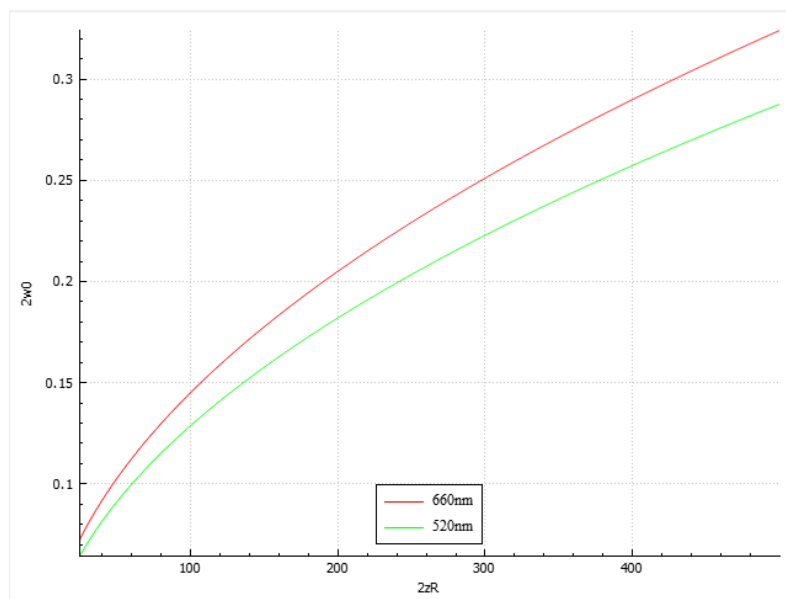


Figure 12. Waist diameter of a Gaussian beam as a function of the Rayleigh length (Donges & Noll, 2015).

above with a triangulation sensor, it is frequently case that the beam diameter within the measurement range should be as small as possible. Then the beam would be formed in such a way (Donges & Noll, 2015):

$$2z_R = M_z \tag{5}$$

where M_z is measuring range of the triangulation sensor in the z-direction (Donges & Noll, 2015).

Results and Discussions

In the previous sections, the mathematical model of the laser triangulation system without Scheimpflug condition has been given and the theoretical results of the system has been shown to prove the system is reliable and robust for 2D/3D measurements.

For the evaluation purpose the components are selected due to the generality in the market. For example, the most stocked industrial camera and objective lens brand is Basler in our country. They can provide the products within two or three days. Table 2 shows the parameters that related to these imaging components and the system general parameters. The results for these parameters for both Lamott and Noll's and our method is given in Figure 10 and 11 respectively.

Table 2. Theoretical application parameters

Name	Unit	Value
Sensor size x	mm	6.6
Sensor size y	mm	4.1
Sensor width	pixels	1920
Sensor height	pixels	1200
Focal length	mm	12
U0	mm	300
d min	mm	100
d max	mm	500
Triangulation angle	degree	50
Field area	mm	200

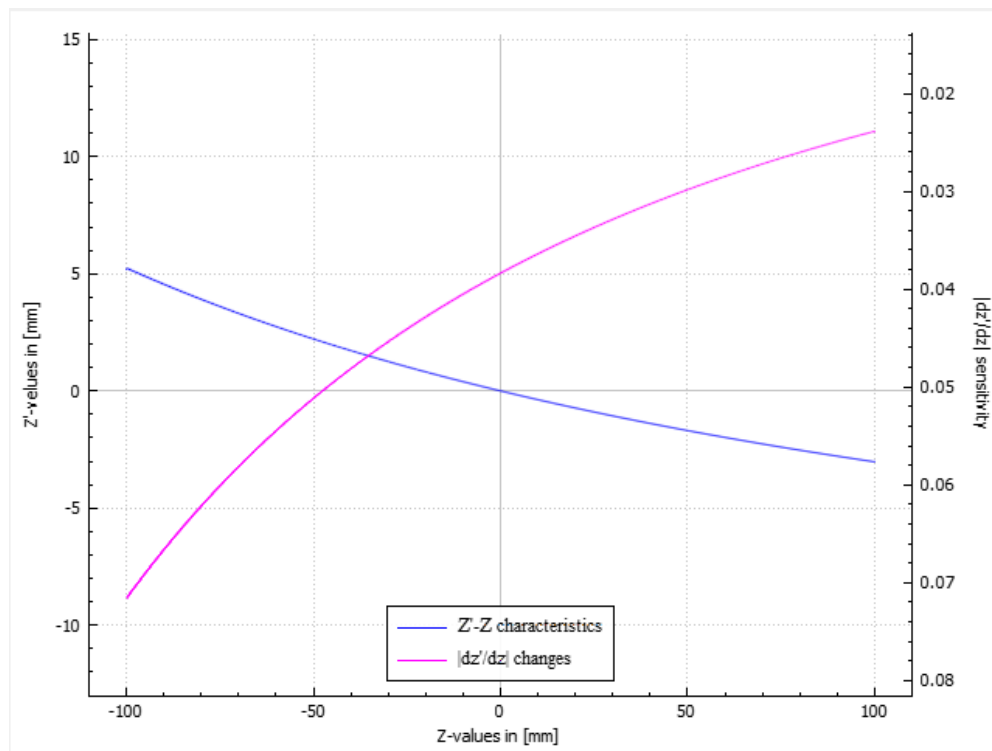


Figure 13. Characteristics curve of the Donges and Noll's system for the parameters that are given in Table 2, $(z'(z))$.

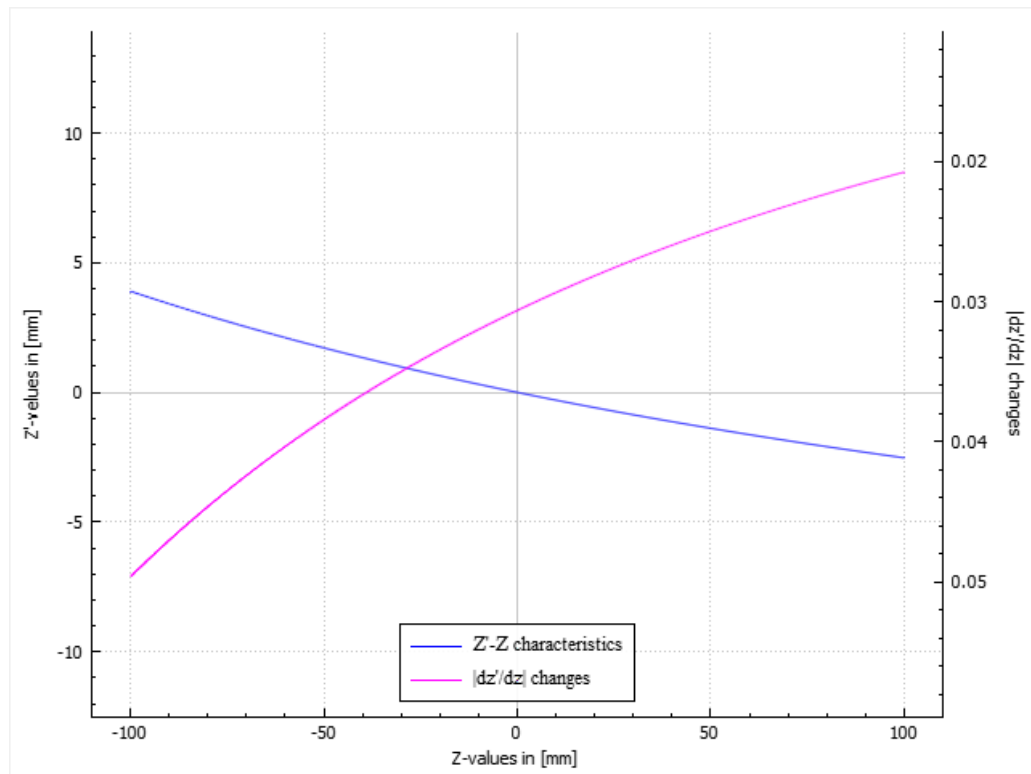


Figure 14. Characteristics curve of our system for the parameters that are given in Table 2, $(z'(z))$.

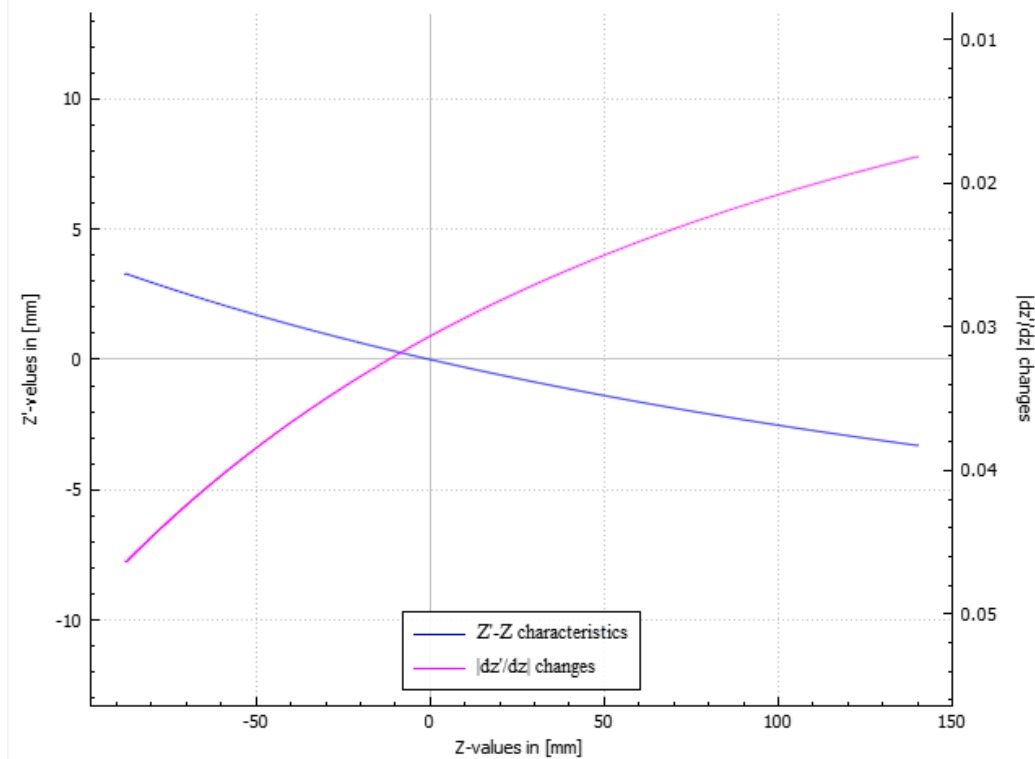


Figure 15. Characteristics curve of our system for the parameters that are given in Table 2, $(z(z'))$.

It can also be seen from Fig. 13 that our system can measure 35mm length when the sensor placed at from 100mm away from the measurement plane and 180mm length when it placed 500mm away from the measurement plane using with our components' and system parameters. When the angle of triangulation is set to 850 within the same parameters given in Table 2, it can be seen that the sensitivity is increasing for Lamott and Noll's model in Fig. 13, while our model is becoming traditional imaging system (Fig. 14).

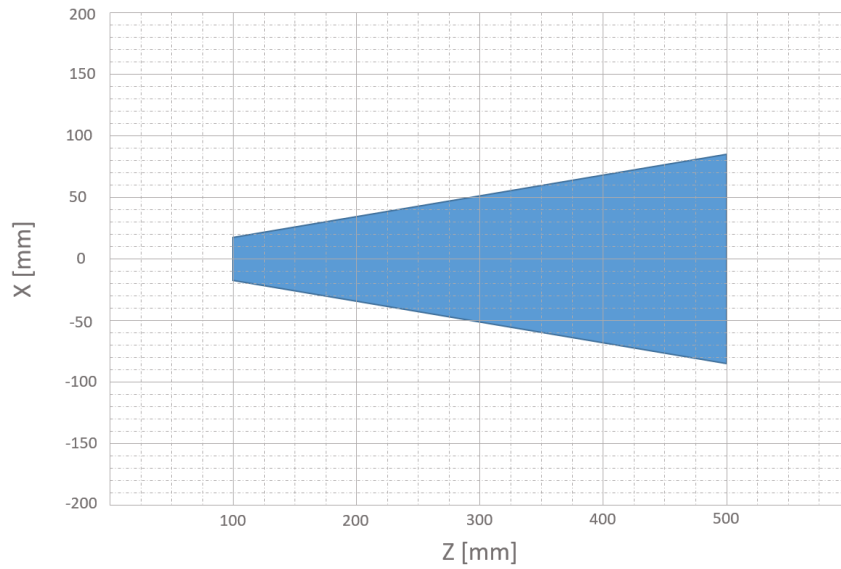


Figure 16. Measurement field for the parameters that are given in Table 2.

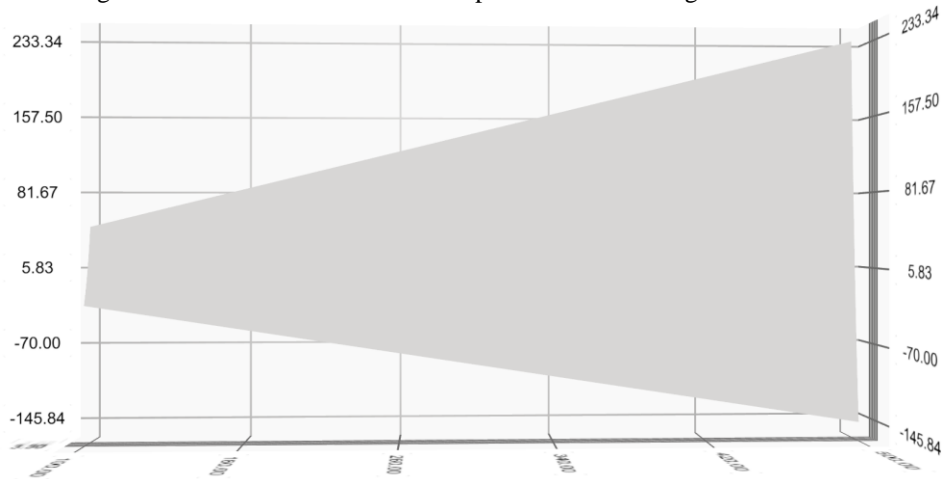


Figure 17. Measurement depth field for the parameters that are given in Table 2.

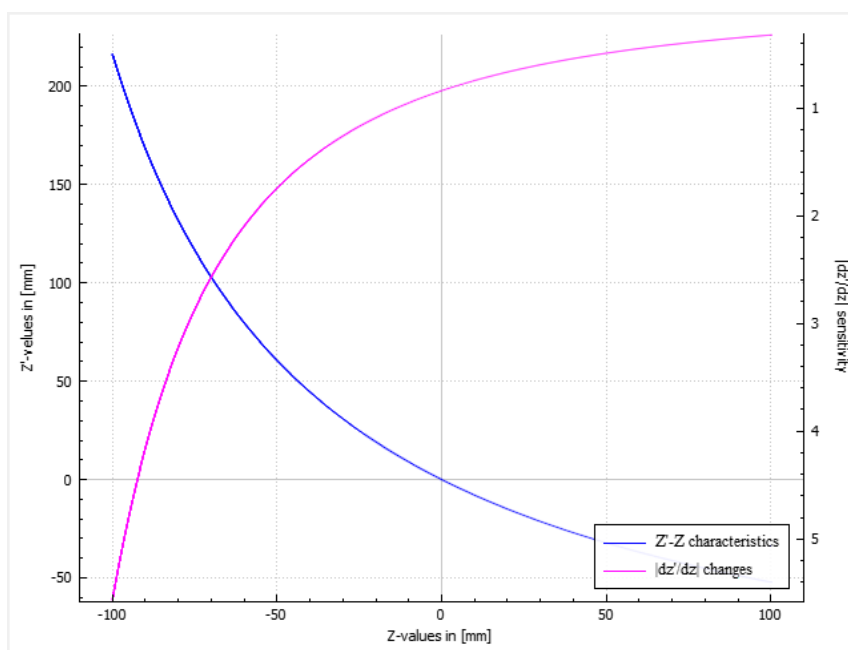


Figure 18. Characteristics curve of the Lamott and Noll's system for the triangulation angle 85° .

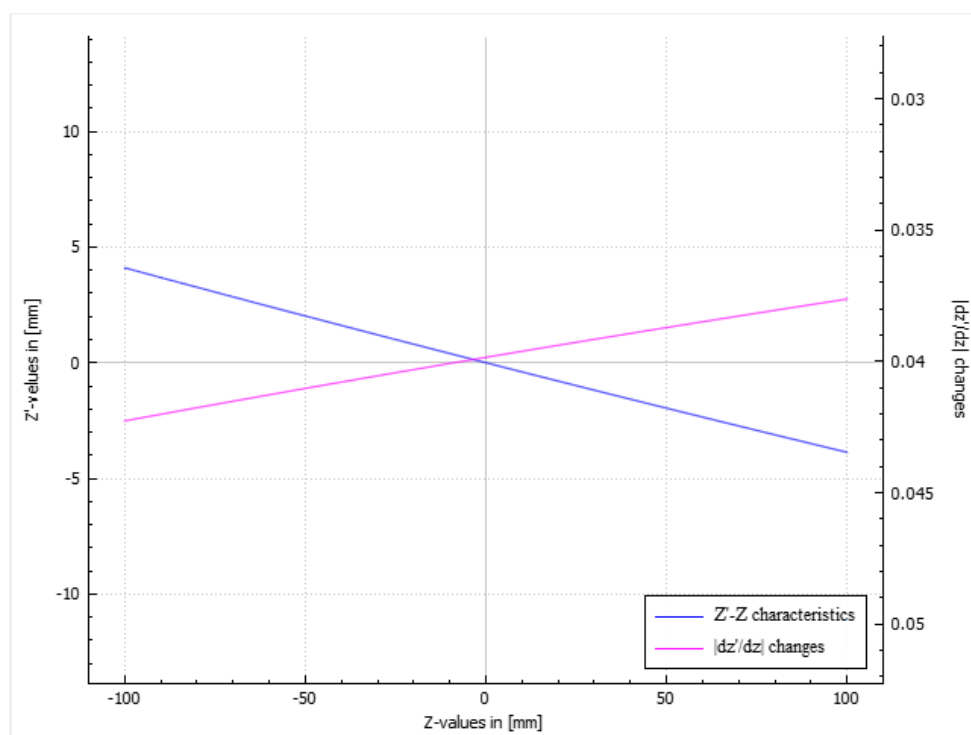


Figure 19. Characteristics curve of our system for the triangulation angle 85° .

Application Examples

Most interesting study about disadvantages of Scheimpflug condition has been proposed in the article by Miks et al. (2013). A detailed analysis of the problem of imaging objects lying in the plane tilted with respect to the optical axis has been performed by means of geometrical optics theory and it has shown that the fulfillment of the Scheimpflug condition does not guarantee the sharp image of the object as it is usually declared because of the fact that due to the dependence of aberrations of real optical systems on the object distance the image becomes blurred.

Poredos et al., have been shown that limitations related to the measuring range and the shadowing effects often lead them to choose a relatively small triangulation angle ($\alpha < 30^{\circ}$). And also they said that the second way to minimize the shadowing effect is the inclusion of a second camera which is symmetrically positioned relative to the laser source to measure in three dimension of human bodies in motion. França et al. have been shown that a 3D scanning system based on low cost laser triangulation and FOV techniques. Their method enables a perfect 3D image reconstruction with high resolution from different angles, colors and depth variation using a video camera (NTCS 4.2~50.4mm, CCD 1/3'') to imaging. Bracun et al. have been presented a new method for a quality assessment of die-castings based on a 3D measurement by a laser triangulation system that has an asymmetrical measuring range and is capable of high resolution measurements. Wu et al., have been presented a non-invasive and non-contact arterial pulsation measurement (APM) system to detect micro-vibration on skin surface based on optical laser triangulation with traditional CMOS camera.

The above examples are based on low cost laser triangulation applications which are not stuck to the Scheimpflug condition. They have shown that results are reliable and the systems are robust. There are also other studies based on the laser triangulation (with and without Scheimpflug condition) method such as measuring inner surfaces of deep holes (Ye et al., 2018) and surface quality assessment of materials (Zhang et al., 2008, Wu et al., 2020, Buschinelli et al., 2014; Bracun et al., 2016), motion correction techniques for moving objects (Goel & Lohami, 2014, Blais et al., 2004; Lindner et al., 2015), form, thickness, profile, liquid level and distance measurements (Lee et al., 2013; Stöbener et al., 2003; Ghiotti et al., 2015; Zhang et al., 2014; Giesko et al., 2007; Dorsch et al., 1994; Buzinski et al., 1992, Dong et al., 2018, Tao and Liu, 2010; Struckmeier et al., 2020; Donadello et al., 2018; Zhuang et al., 1994; Molleda et al., 2010; Lombardo et al., 2000; Baozhen et al., 2013; Demeyere et al., 2007), reverse engineering (Cajal et al., 2015), laser radar applications (Busk & Heiselberg, 2004) and simulation analysis (Cajal et al., 2015).

Conclusion

Study of this paper shows that the laser triangulation model without Scheimpflug condition is nearly results same with traditional model with some restrictions such as angle and sensor limitations. Also, taking consider the relationship between beam waist diameter at the Rayleigh length, it can be seen from Fig. 16 that the laser beam waist should be fixed within the measuring range. A desktop application is developed to ensure that the system is theoretically satisfying the requirements of measurements via C++ and open source Qt Framework.

In the future works, the system will be built in the laboratory and image acquisition and processing will be done with parallel on one of the up-to-date NVIDIA embedded boards. Also, the custom 3D data plotting section of the application code will be shared as an open source.

Scientific Ethics Declaration

The authors declare that the scientific ethical and legal responsibility of this article published in EPSTEM journal belongs to the authors.

Acknowledgements or Notes

* This article was presented as oral presentation at the International Conference on Basic Sciences, Engineering and Technology (www.icbasnet.net) held in Marmaris/Turkey on April 27-30, 2023.

* This study is supported by management of Baykal Machinery. Thanks to all our managers.

* Qt is the trademark of the Qt Company Ltd.

References

- Bracun, D., Gruden, V., & Mozina, J. (2008). A method for surface quality assessment of die-casting based on laser triangulation. *Measurement Science and Technology*, 19(4), 045707.
- Cajal, C., Santolaria, J., Samper, D., & Garrido, A. (2015). Simulation of laser triangulation sensors scanning for design and evaluation purposes. *International Journal of Simulation Model*, 14(2), 250 – 264.
- Donges, A., & Noll, R. (2015). *Springer series in optical sciences - laser measurement technology: Fundamentals and applications* Volume 188. (pp. 247 – 279), Springer.
- França, J. G. D. M., Gazziro, M. A., Ide, A. N., & Saito, J. H. (2005). A 3d scanning system based on laser triangulation and variable field of view. *IEEE International Conference on Image Processing 2005*, 1 , (p.425).
- Lamott, A., & Noll, R., (2011). *Tailored light 2 – laser application technology (RWTH ed.)*. (pp .473 – 537). Springer.
- Poredoš, P., Povšič, K., Novak, B., Jezeršek, M. (2015), Three-dimensional measurements of bodies in motion based on multiple laser-plane triangulation. *Revista Technica de la Facultad de Ingenieria Universidad del Zulia*, 38(2), 53-61.
- Ye, Z., Lianpo, W., Gu, Y., Chao, Z., Jiang, B., & Ni, J. (2018). A laser triangulation-based 3D measurement system for inner surface of deep holes. *Proceedings of the ASME 2018 : 13th International Manufacturing Science and Engineering Conference*, Texas, USA.
- Zhang, L., Zhao, M., Zou, Y., & Gao, S. (2008). A new surface inspection method of TWBS based on active laser triangulation. *7th World Congress of Intelligent Control and Automation*. China.
- Wu, J. H., Chang, R. S., & Jiang, J. A. (2007). A novel pulse measurement system by using laser triangulation and a CMOS image sensor. *Sensors 2007*, 7, 3366 – 3385.
- Tong, Q., Jiao, C., Huang, H., Li, G., Ding, Z., & Yuan, F. (2014). An automatic measuring method and system using laser triangulation scanning for the marameters of a screw thread. *Measurement Science and Technology*, 25.
- Donadello, S., Motta, M., Demir, A. G., & Previtali, B. (2018). Coaxial laser triangulation for height monitoring in laser metal deposition. *10th CIRP Conference on Photonic Technologies [LANE 2018]*, 144 – 148.
- Baozhen, G., Jingbin, S., Pengcheng, L., Qieni, L., & Di, W. (2013). Designing an optical set-up of differential laser triangulation for oil film thickness measurement on water. *Review of Scientific Instruments*, 84.

- Miks, A., Novak, J., & Novak, P. (2013). Analysis of imaging for laser triangulation sensors under Scheimpflug rule. *OSA 2013*, 21(15).
- Predoš, P., Čelan D., Možina, J., & Jezeršek, M. (2015). Determination of the human spine curve based on laser triangulation. *BMC Medical Imaging*, 15(2).
- Demeyere, M., Rurimunzu, D., & Eguène, C. (2007). Diameter measurement of spherical objects by laser triangulation in an ambulatory context. *IEEE Transactions on Instrumentation and Measurement*, 57, 867 – 872.
- Stöbener, D., Dijkman, M., Kruse, D., Surm, H., Keßler, O., Mayr, P., & Goch, G. (2003). Distance measurements with laser triangulation in hot environments. *XVII IMEKO World Congress*, 1898 – 1902.
- Ghiotti, A., Schöch, A., Salvadori, A., Carmignato, S., & Savio, E. (2015). Enhancing the accuracy of high-speed laser triangulation measurement of freeform parts at elevated temperature. *CIRP Annals – Manufacturing Technology*, 64, 499 – 502.
- Zhang, H., Ren, Y., Liu, C., & Zhu, J. (2014). Flying spot laser triangulation scanner using lateral synchronization for surface profile measurement. *Applied Optics*, 53(20), 4405 – 4412.
- Koch, T., Breier, M., Li, W. (2013). *2013 11th IEEE International Conference on Industrial Informatics*. 48 – 53.
- Mikhlyayev, S. V. (2006). Influence of a tilt of a mirror surface on the measurement accuracy of laser triangulation rangefinder. *Journal of Physics: Conference Series, International Symposium on Instrumentation Science and Technology*, 48, 739 – 744.
- Giesko, T., ZBrowski, A., Czajka, P. (2007). Laser profilometers for surface inspection and profile measurement. *Problemy Eksploatacji*, 97-108.
- Buschinelli, P., Pino, T., Silva, F., Santos, J., & Albertazzi, A. (2015). Laser triangulation profilometer for inner surface inspection of 100 millimeters (4”) nominal diameter. *Journal of Physics: 3rd International Congress on Mechanical Metrology*, 648.
- Dong, Z., Sun, X., Liu, W., & Yang, H. (2018). Measurement of free-form curved surfaces using laser triangulation. *Sensors 2018*, 18(10). 3527.
- Tao, H., & Liu, W. (2010). Measurement system for liquid level based on laser triangulation and angular tracking. *Journal of Computers*, 5(9), 1444 – 1447.
- Ehlert, E., Horn, H. J., & Adamek, R. (2008). Measuring crop biomass density by laser triangulation. *Computer and Electronics in Agriculture*, 61(2), 117 – 125.
- Molleda, J., Usamentiaga, R., Garcia, D. F., & Bulnes, F. G. (2010). Real-time flatness inspection of rolled products based on optical laser triangulation and three dimensional surface reconstruction. *Journal of Electronic Imaging*, 19(3), 031206-031206.

Author Information

Orkun KASAPOGLU

Baykal Machinery

Bursa, Turkey

Contact e-mail: orkunk@baykal.com.tr**Tugba BILGIN**

Baykal Machinery

Bursa, Turkey

To cite this article:

Kasapoglu, O. & Bilgin, T. (2023). Mathematical analyzing of laser triangulation system without Scheimpflug condition via C++ and Qt framework. *The Eurasia Proceedings of Science, Technology, Engineering & Mathematics (EPSTEM)*, 22, 1-14.